*Pharmaceutical Research, Vol. 7, No. 2, 1990*

*Research Article*

# Transport Mechanisms in Iontophoresis. I. A Theoretical Model for the Effect of Electroosmotic Flow on Flux Enhancement in Transdermal Iontophoresis[1]

**Michael J. Pikal[2]**

*Received March 20, 1989; accepted August 1, 1989*

Bulk fluid flow or volume flow in the direction of counterion flow is a probable mechanism for enhanced flux of uncharged species by iontophoresis. Both the electrical volume force effect, resulting from the interaction of the "ion atmosphere" and the electric field, and an induced osmotic pressure effect produce volume flow in the same direction as counterion flow through the membrane. Since each of these effects is proportional to the membrane charge and the imposed electric field, we classify both as electroosmotic flow. This research develops a detailed theoretical model which allows the effect of volume flow on flux enhancement to be evaluated. A detailed theoretical result for the electroosmotic flow coefficient also results from the analysis. The model assumes that transport occurs in three types of aqueous pores: positively charged, neutral, and negatively charged. For hairless mouse skin (HMS), pore size, charge, and number are evaluated from transference number, volume flow, and electrical resistance data. The flux enhancement ratio is $J_1/J_1^D = \Sigma A_i\alpha_i/[1 - \exp(-\alpha_i)]$, where $i$ = pore type, and the summation runs over the three pore types. $A_i$ is the area fraction of pore type $i$ effective for transport; $J_1$ and $J_1^D$ are flux of species 1 with and without the electric field, respectively; and $\alpha_i$ is given by $\alpha_i = F(-\Delta\Phi/RT)[z_1 + (-z_m^i)Bar_i^2C_m^i(G_i + F)]$. Here $F$ = Faraday's constant; $-\Delta\Phi$ = voltage drop; $R$ = gas constant; $T$ = absolute temperature; $z_m^i$ = charge of pore $i$; $C_m^i$ = charge concentration in membrane pore of radius, $r_i$; $B$ is a known collection of constants; $a$ is the Stokes radius of the transported solute; $G_i$ is a function of membrane charge and pore radius coming from the electrical volume force effect; and $F$ is a function of membrane charge and ion mobility arising from the induced osmotic pressure effect. For transdermal iontophoresis, $F<<G$, and the induced osmotic pressure effect is not significant. Negative pores dominate electroosmotic flow and usually dominate flux enhancement. The term proportional to $C_m^i$ is the contribution of electroosmotic flow and will always increase the flux enhancement ratio for anodic delivery of a positively charged ion ($z_1 > 0$) or a neutral species ($z_1 = 0$) in a negatively charged pore. The theoretical results are consistent with data in the literature.

**KEY WORDS:** transdermal; iontophoresis; electroosmosis; volume flow; mechanisms of iontophoresis; theory of iontophoresis.

## INTRODUCTION

Iontophoresis normally refers to the transfer of ionic solutes through biological membranes under the influence of an electric field (1). Pharmaceutical interest has concentrated on transdermal iontophoresis, where numerous studies have shown considerable enhancement of transport via iontophoresis over that observed in conventional transdermal or "passive" transport of the same compounds (1). The traditional interpretation holds that the increased transport is a direct result of the increased driving force resulting from the action of the electric field on the ionic solute. However, Gangarosa and co-workers (2) have observed increased transport of nominally neutral species[3] by application of an electric field, and later work by Burnette and co-workers demonstrated enhanced transport of neutral thyrotropin releasing hormone (3) and mannitol (4) when delivered from the anode compartment of the apparatus. Electroosmotic flow was suggested as a possible mechanism responsible for the transport of neutral species (2–4), but no quantitative statements could be made due to lack of a satisfactory theoretical model for flux enhancement via electroosmotic flow.

When an electrical potential difference is applied across a "porous" membrane containing fixed charges (i.e., ionic groups immobilized in the membrane), bulk fluid flow occurs in the direction of counterion migration (5–7). Mechanisti-

[1] Presented, in part, at the 1st National Meeting of the AAPS, Washington, D.C., November 1986.

[2] Lilly Research Laboratories, Eli Lilly & Co., Indianapolis, Indiana 46285.

[3] While pH changes at the electrodes during electrolysis resulted in ionization of the nominal neutral species in some experiments, their conclusions remain valid for delivery of water, anodic delivery of thymidine, and cathodic delivery of ARA-A.

0724-8741/90/0200-0118$06.00/0 

cally, both the electrical volume force on the "ion atmosphere" and the induced osmotic pressure effect discussed by Barry and Hope (8,9) contribute to the observed volume flow. Under conditions of equal temperature, hydrostatic pressure, and solution composition on both sides of the membrane, the volume flow, $J_v$, in units of volume time$^{-1}$ area$^{-1}$, is directly proportional to the electric field or, alternately, directly proportional to the negative of the potential gradient, $-d\Phi/dx$ (5),

$$J_v = L_{VE}(-d\Phi/dx) \quad (1)$$

where $L_{VE}$ is a phenomenological coefficient describing the direction and magnitude of the volume flow resulting from the driving force, $-d\Phi/dx$. Equation (1) is the phenomenological definition of electroosmotic flow, with $L_{VE}$ being the electroosmotic flow coefficient. Since both mechanisms mentioned above produce volume flow in accord with Eq. (1), both effects produce electroosmotic flow. Note that the sign convention gives positive volume flow when the counterions are positive (i.e., the membrane is negative).

Since a neutral species is part of the fluid, it will be transported with the fluid, although some or all of the solute may be filtered or "reflected" from the fluid flowing through the pores by a sieve mechanism (6,7). Near-zero reflection would be expected for small molecules, but for molecules larger than the pore size, reflection would nominally be 100% (6). Our interest is in the contribution of volume flow to the flux enhancement ratio, $J_1/J_1^D$, where $J_1$ is the flux of species 1 during iontophoresis, and $J_1^D$ is the corresponding flux in the absence of an electric field ("passive transport"). Since, as a first approximation, solute "reflection" will reduce both $J_1$ and $J_1^D$ in a given pore by the same factor, calculation of the flux enhancement ratio for a single pore does not involve the complexity of estimating solute reflection.

The solution containing species 1 is presumed to also contain supporting electrolyte (i.e., buffers and other salts such as NaCl) *which carries most of the current*. The opposite case, where the drug is an electrolyte which carries most of the current, is a much simpler theoretical problem which is addressed briefly under Discussion.

Previous theoretical treatments either have evaluated the flux enhancement ratio *without the electroosmotic flow contribution* (10) or have evaluated only the *formal* effect of electroosmotic flow on the flux equations without addressing a quantitative estimate of the effect on flux enhancement (3). The main objective of the present research is to present a more detailed theoretical analysis which will permit, with evaluation of key parameters from experimental data, a quantitative estimate of the effect of electroosmotic flow on flux enhancement via iontophoresis. Secondarily, the resulting molecular theory for electroosmotic flow allows an assessment of the relative importance of the two mechanisms for electroosmotic flow. Separate reports address the experimental determination of volume flow in hairless mouse skin (11) and the experimental flux enhancement ratios for neutral species and polymeric anions (12).

## Phenomenological Theory for Flux Enhancement Ratio

This section develops the formal relationship between flux enhancement and electroosmotic flow using a simple model which treats iontophoresis as equivalent to mass transfer through a collection of aqueous channels or pores. The analysis is basically an extension of previous treatments (3,10).

We focus on transport in a given pore or channel. Following conventional nonequilibrium thermodynamics (13), the steady-state flux of species 1 relative to the solvent, $j_1$, is linearly related to the conjugate forces, $X_j$, through the Onsager transport coefficients, $l_{1j}$, by the relationship,

$$j_1 = \Sigma l_{1j} X_j, \quad (2)$$

where the summation over $j$ extends over all components in the system including the species of interest, component 1, the counterions and co-ions from the supporting electrolyte (components 2 and 3, respectively), and the membrane (or pore) itself. The supporting electrolyte is typically NaCl. Note that the solvent fixed flow, $j_1$, measures flow velocity relative to the solvent, $j_1 = \underline{c}_1(v_1 - v_0)$, where $\underline{c}_1$ is the concentration of component 1 (mol/cm$^3$) in the membrane "pore," and the velocities $v_1$ and $v_0$ are flow velocities of component 1 and water, respectively, measured relative to the membrane. The solvent fixed flux, $j_1$, is related to the corresponding flux measured relative to the membrane, $J_1$, by

$$j_1 = J_1 - (\underline{c}_1/\underline{c}_0)J_0 \quad (3)$$

The volume flow, $J_v$, is the solvent velocity, $v_0$, which in turn is equal to the ratio, $J_0/\underline{c}_0$. The thermodynamic forces, $X_j$, are given by the gradients of the electrochemical potentials,

$$X_j = -[\partial\mu_j/\partial x + z_j F\partial\Phi/\partial x] \quad (4)$$

where $\mu_j$ is the chemical potential of component $j$ given in terms of the standard-state chemical potential, $\mu_j^0$, the concentration, $\underline{c}_j$, and the activity coefficient, $\gamma_j$,

$$\mu_j = \mu_j^0 + RT \ln \underline{c}_j \gamma_j \quad (5)$$

where $R$ is the gas constant, and $T$ is the absolute temperature. In Eq. (4), distance is symbolized by $x$, $F$ is Faraday's constant, $z_j$ is the signed valence of species $j$, and $\Phi$ is the electrical potential.

To obtain a tractable model, we assume, consistent with previous workers (3,10), that $l_{1j} = 0$ for $j \neq 1$ and further assume that activity coefficients are independent of distance, $x$. While the latter assumption should be a good approximation if the concentration of species 1 is low compared to the concentration of other species, which will often be the case of practical interest, the assumption $l_{1j} = 0$ ($j \neq 1$) is more serious and essentially assumes that the interaction between component 1 and component $j$ is much less than the interaction between component 1 and the solvent, which is measured by $l_{11}$ (13,14). In *dilute* electrolytes, where $l_{11} >> l_{1j} (j \neq 1)$, the neglect of $l_{1j} (j \neq 1)$ is a good first approximation (13,14). Thus, the model is essentially equivalent to assuming that iontophoresis occurs in large pores filled with dilute aqueous electrolyte having trace levels of component 1. Ignoring the interaction of component 1 with the membrane (i.e., $l_{11} >> l_{1m}$) would appear to be the most serious approximation, particularly if the size of component

1 was of the same order of magnitude as the pore size. However, as indicated earlier, interaction with the membrane would retard both the iontophoretic flux, $J_1$, and the "passive flux," $J_1^D$, by approximately the same factor and would, as a first approximation, cancel in the flux enhancement ratio.

Subject to the above approximations, combination of Eq. (1) and Eqs. (2)–(5) yields

$$J_1 = -D_1^*(\partial \underline{c}_1/\partial x) - \underline{c}_1(D_1^* z_1 F/RT + L_{VE})\partial\Phi/\partial x \quad (6)$$

where the relationship (14), $D_1^* = RTl_{11}/\underline{c}_1$, has also been used to replace the Onsager transport coefficient by the tracer diffusion constant, $D_1^*$. Note that $D_1^*$ represents the diffusion of component 1 in an electrolye solution of the same composition as the pore fluid and does not include interaction with the membrane.[4] Equation (6) is essentially the Nernst–Planck flux equation modified to include the effect of volume flow on transport.

Evalulation of $J_1$ requires $\underline{c}(x)$, which may be evaluated from Eq. (6) if we assume Ohms law and a position-independent specific resistance in the pore fluid, the latter being consistent with the model if component 1 is a tracer species. Steady-state current flow demands that $\partial\Phi/\partial x$ be a constant, while steady-state flux of 1 demands that $\partial J_1/\partial x = 0$. Thus, differentiation of Eq. (6) with respect to $x$ and substitution of $\Delta\Phi/L = \partial\Phi/\partial x$, where $L$ is the pore length, yields

$$\partial^2 \underline{c}_1/\partial x^2 - B\partial \underline{c}_1/\partial x = 0 \quad (7)$$

$$B = [z_1F/RT + L_{VE}/D_1^*](-\Delta\Phi/L) \quad (8)$$

Solution of Eq. (7) subject to the boundary conditions, $\underline{c}_1(x = 0) = \underline{c}_1^\circ$, $\underline{c}_1(x = L) = 0$, gives $\underline{c}_1(x)$, which then is used to evaluate $\partial \underline{c}_1/\partial x$ in Eq. (6). The flux enhancement ratio for a given pore is then given by

$$J_1/J_1^D = \alpha/[1 - \exp(-\alpha)] \quad (9)$$

where $J_1$ is the pure diffusion or "passive" term, $\underline{c}_1^\circ D_1^*/L$, and $\alpha$ is given by

$$\alpha = [z_1F/RT + L_{VE}/D_1^*](-\Delta\Phi) \quad (10)$$

The flux enhancement ratio is similar to previous results (10), differing only in that the effect of volume flow is included by the term in $L_{VE}$.

### Theoretical Evaluation of the Electroosmotic Flow Coefficient $L_{VE}$

The coefficient, $L_{VE}$, represents volume flow due to two effects: (a) the electrical volume force on the ion atmosphere and (b) the induced osmotic pressure effect discussed by Barry and Hope (8,9). A schematic of the capillary pore model used to evaluate these effects is given in Fig. 1. The membrane pore is lined with fixed or immobile charges, assumed negative in this example. The ion atmosphere (15) is the region in the pore fluid which contains a nonzero charge density, $\rho$, arising from mobile ions, which when integrated over the total volume of the pore must be equal in magnitude but opposite in sign to the total fixed charge on the pore wall. While the schematic shows a definite thickness, $1/\kappa$, for the ion atmosphere (i.e., the charge density is zero farther than $1/\kappa$ from the wall), the ion atmosphere actually dissipates continuously with increasing distance from the pore wall. Interaction of the electric field with the ion atmosphere produces an electrical volume force of magnitude, $\rho E$, which is a driving force for electroosmotic flow (15,16).

Due to Donnan exclusion, the counterion transference number in a charged membrane is higher than the corresponding transference number in aqueous solution (6). Barry and Hope (8,9) have shown that the discontinuity in counterion transference number which exists at the phase boundary between external solution and membrane causes effective concentration polarization at the phase boundaries, which results in an induced osmotic pressure driving force, $\Delta\pi/L$. These two forces, electrical volume and induced osmotic, are balanced by viscous forces and produce volume flow in the same direction as flow of counterions. The induced osmotic pressure force is time dependent but reaches steady state quickly (8,9). Note that while the electrical volume force depends on distance from the pore wall, the induced osmotic force is independent of position.

The combined effect of the two forces is evaluated by a hydrodynamic analysis similar to that given by Bird *et al.* (17) for fluid flow in a capillary tube under the influence of a pressure difference and a gravitational field. We simply substitute osmotic pressure difference, $\Delta\pi$, for pressure difference, charge density for density, and electric field for the gravitational constant and proceed using essentially the same mathematical procedure. Using the Gouy–Chapman approximation (15) to evaluate the charge density and assuming that the pore radius, $r_p$, is large compared to the mean thickness of the ion atmosphere, $1/\kappa$, yields

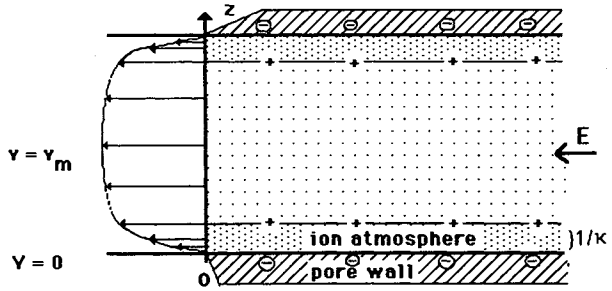


Fig. 1. Schematic of the electrical double layer in a pore and the fluid velocity distribution in electroosmotic flow. The length of the arrows denote the magnitude of the fluid velocity, v. The fluid velocity is zero at the pore wall and increases toward a maximum at the tube center. The pore wall has immobile negative charges, and the ion atmosphere, of thickness $1/\kappa$, has a net positive charge. The electric field, $E$, interacts with the positively charged fluid (ion atmosphere) to produce a force on the fluid in the ion atmosphere and, also, produces an induced osmotic pressure force on all the pore fluid. These forces are balanced by a viscous force, i.e., $dv/dz \neq 0$.

[4] Modification of Eq. (6) to include strong interaction of component 1 with the membrane would involve introduction of the reflection coefficient, $\sigma$, as the factor $(1 - \sigma)$ multiplying $J_0$ in Eq. (3). The tracer diffusion coefficient in the pore fluid, $D_1^*$, would also be multiplied by the factor $(1 - \sigma)$ to adjust the diffusional mobility for strong interaction with the membrane. The net effect on Eq. (6) would then involve multiplication of $D_1^*$ and $L_{VE}$ by the factor $(1 - \sigma)$. Since the relection coefficient term would cancel in the calculation of the flux enhancement ratio, this term is omitted from our analysis.

$$J_v = v_\pi + v\rho \quad (11)$$

where $v_\pi$ is the volume flow contribution from the Barry and Hope induced osmotic pressure effect,

$$v_\pi = (k_\pi r_p^2/8\eta L)(-\Delta\Phi_v) \quad (12)$$

with $k_\pi$ being defined in terms of the osmotic pressure difference, $\Delta\pi$,

$$\Delta\pi = k_\pi(-\Delta\Phi_v) \quad (13)$$

and $v_\rho$ is the contribution of the electrical volume force,

$$v_\rho = [F\ 10^4(-z_m)r_p^2 C_m G(\kappa r_p/2)/4\eta L](-\Delta\Phi_v) \quad (14)$$

where $G(\kappa r_p/2)$ is a function of the dimensionless group, $\kappa r_p/2$. For a large pore radius (i.e., $\kappa r_p/2 >> 1$), $G(\kappa r_p/2) \approx (\kappa r_p/2)^{-1}$. Other symbols in Eqs. (12)–(14) are defined as follows: $F$ is Faraday's constant in coulombs per equivalent, $z_m$ is the signed valence of the fixed membrane charges, $C_m$ is the membrane charge concentration in equivalents of fixed charges per liter of pore volume, $\eta$ is the viscosity of the pore fluid, and $\Delta\Phi_v$ is the potential difference across the membrane in volts. The mean radius of the ion atmosphere is related to the ionic strength in the pore, which assuming univalent salts and univalent fixed charges, becomes (15)

$$\kappa = A(C_m + \underline{C})^{1/2} \quad (15)$$

where $\underline{C}$ is the concentration of co-ions (or salt) in the pore in moles per liter, and $A$ is a constant, which for water at 35°C is $3.3\ 10^7\ cm^{-1}$.

Our result for the electrical volume force contribution to volume flow is self-consistent only when the pore radius is large compared to the thickness of the ion atmosphere. The more sophisticated derivation given by Manning (16) for electroosmotic flow *in the absence of the induced osmotic pressure effect* does not suffer from this limitation. Note that our results [Eq. (11)] indicate that the electrical volume force and induced osmotic effects are additive. Assuming that additivity would be preserved in a more sophisticated treatment of the combined effects, we may use the Manning result for the electrical volume force contribution, resulting in a self-consistent result for $G(\kappa r_p/2)$ regardless of the thickness of the ion atmosphere, thereby giving

$$G(y) = [\coth(y) - 1/y]/y \quad (16)$$

where $y = \kappa r_p/2$. Note that for large $y$, $G(y)$ approaches $1/y$, and for small $y$, $G(y)$ approaches ⅓.

We now consider the evaluation of $k_\pi$. Barry and Hope (8) show that the steady-state osmotic pressure difference, $\Delta\pi$, is given in terms of the current density, $i$, by

$$\Delta\pi = 4\Delta t_2 i\tau(1 + \beta\tau)^{-1}/F(D^\circ/RT) \quad (17)$$

where $\Delta t_2$ is the difference in counterion transference number between the membrane phase and the aqueous solution phase, $\tau$ is the thickness of the unstirred aqueous boundary layer, and $D^\circ$ is the electrolyte diffusion coefficient in bulk solution. The term, $\beta$, is defined by the expression, $\beta = 4\omega RT/D^\circ$. Here, $\omega$ is a membrane permeability coefficient defined by

$$J_s = 2RT\omega\Delta c \quad (18)$$

Equation (18) is essentially a diffusion equation relating the flux of electrolyte, $J_s$, to the concentration difference, $\Delta c$, (in moles/cm$^3$) between the solutions in contact with the membrane. Using irreversible thermodynamics (11) to relate $i/D^\circ$ to transference numbers and potential difference, $\Delta\Phi$, the constant, $k_\pi$, may be written[5]

$$k_\pi = (2 \cdot 10^4 F)(f\tau/\eta_r L)(1 + \beta\tau)^{-1}(\Delta t_2/t_2^\circ t_3^\circ) \times (t_2^\circ C_m + \underline{C}), \quad (19)$$

where $\underline{C}$ is the concentration of co-ions (mol/liter) in the pore, $t_2^\circ$ and $t_3^\circ$ are transference numbers of counterion and co-ion in the external solution, and $\Delta t_2$ is the difference between transference numbers of counterion in the membrane, $t_2$, and in the external solution, $t_2^\circ$, $\Delta t_2 = t_2 - t_2^\circ$. The relative viscosity of the fluid in the pore, $\eta_r$, enters from our use of the Stokes–Einstein relationship to relate ionic mobility in a pore to mobility in the external solution where the viscosity is essentially that of pure water. The parameter, $f$, is the fraction of total membrane area which is pore area.

Similarly, $\beta\tau$ may be written

$$\beta\tau = K_{23}(f\tau/\eta_r L)[(C_m + 2\underline{C})/(C_m + \underline{C})](t_2/t_2^\circ) \quad (20)$$

The membrane solution electrolyte distribution coefficient, $K_{23}$, is defined by $K_{23} = \underline{C}/C$, where $C$ is the concentration in the external solution as moles per liter. As a first approximation, consistent with our pore model,[6] $K_{23}$ may be written (6)

$$K_{23} = (C_m/2C)\{[1 + (2C/C_m)^2]^{1/2} - 1\} \quad (21)$$

Note that $K_{23}$ is also the distribution coefficient for the co-ion. Equations (19) and (20) contain implicit dependencies on $C_m$ through the transference numbers. We now express the transference numbers in terms of $C_m$ to obtain an expression explicit in $C_m$ dependence. Since the transference number of species $i$ is proportional to the product of the concentration of that ion, $\underline{C}_i$, and its single ion conductivity, $\lambda_i$, we may write

$$t_2 = \lambda_2(C_m + \underline{C})/[\lambda_2(C_m + \underline{C}) + \lambda_3\underline{C}] \quad (22)$$

since the single ion conductivity of the fixed charge is zero. As a first approximation, we assume that the *ratio* of ionic mobilities in the membrane phase is the same as the corre-

[5] Our derivation is developed from a description of transport phenomena in terms of membrane fixed Onsager transport coefficients, $L_{ij}$. Consistent with our model, we take $L_{ij} = 0$ $(i \neq j)$, but the result given in Eq. (19) is probably independent of this assumption. We also assume, consistent with Barry and Hope, that the electrolyte concentration in the unstirred layer is constant in planes parallel to the membrane surface. This assumption is fully consistent with a pore model for membrane transport only if lateral diffusion between pore openings is fast compared to diffusion through the unstirred layer, i.e., if the distance between pores is small compared to the thickness of the unstirred layer. Based on estimated values for pore area fraction and mean pore size (discussed later), we estimate that the mean distance between pores is at least one order of magnitude less than the thickness of the unstirred layer in typical transdermal iontophoresis applications.

[6] Equation (21) may be obtained from Eq. 117 in Ref. 6 assuming that the "free energy of swelling" is negligible and assuming that the mean activity coefficient in the capillary pore is the same as the mean activity coefficient in the external solution.

sponding ratio in the external electrolyte solution, $\lambda_i/\lambda_j = \lambda_i^\circ/\lambda_j^\circ$, giving

$$k_\pi = (2 \cdot 10^4 F)(f\tau/\eta_r L)C_m(1 + \beta\tau)^{-1} \quad (23)$$

with $\beta\tau$ given by

$$\beta\tau = K_{23}(f\tau/\eta_r L)(C_m + 2\underline{C})/(t_2^\circ C_m + \underline{C}) \quad (24)$$

Combination of Eqs. (1), (11), (12), (14), and (23) then gives the final result for the electroosmotic flow transport coefficient, $L_{VE}$, as units of $cm^2\ sec^{-1}\ V^{-1}$,

$$L_{VE} = [10^4 F r_p^2(-z_m)C_m/4\eta][G(\kappa r_p/2) + (f\tau/\eta_r L)(1 + \beta\tau)^{-1}] \quad (25)$$

The term in $G$ represents the electrical volume force contribution, and the term involving the unstirred layer thickness, $\tau$, represents the Barry and Hope induced osmotic pressure contribution.

Note that $L_{VE}$ given by Eq. (25) is the electroosmotic flow transport coefficient for a given pore. The corresponding "experimental" coefficient for the membrane as a whole, $L_{ve}$, may be defined in terms of total volume flow, $J_v$, as $\mu l/hr\ cm^2$, by the expression $J_v = L_{ve}(-\Delta\Phi)$. Here volume flow is normalized with respect to the total membrane area. In a membrane which is a collection of many identical pores, with a ratio of pore area to total area denoted, $f$, the relationship between $L_{VE}$ and the experimental transport coefficient, $L_{ve}$, as $\mu l\ cm^{-2}\ hr^{-1}\ V^{-1}$, is given by

$$L_{ve} = 3.6 \cdot 10^6(f/L)L_{VE} \quad (26)$$

where $L$ is the pore length.

An expression for volume flow, $J_v$, in terms of current density is useful since data are typically obtained at constant current. The development of this expression proceeds by first using "Ohm's law" to write the voltage drop, $(-\Delta\Phi)$, in terms of current density, $i$, and area-normalized resistance, $R'$: $(-\Delta\Phi) = iR'$. The electrical resistance, $R'$, is given by $R' = (L/f)\rho_r$, where $L$ is the pore length, $f$ is the pore area fraction, and $\rho_r$ is the specific resistance of the pore fluid, which may be related to the single ion equivalent conductance, $\lambda_i$, and ion concentrations in the pores,

$$\rho_r = 1000/[\lambda_2(C_m + \underline{C}) + \lambda_3\underline{C}] \quad (27)$$

Consistent with previous assumptions, we assume that the single ion conductance at a given ionic strength is inversely proportional to the viscosity of the medium. This approximation allows the single ion conductance in the pore fluid to be related to the corresponding conductance in the external electrolyte, $\lambda_i$, by, $\lambda_i = \lambda_i^\circ/\eta_r$, where $\eta_r$ is the relative viscosity of the pore fluid. Algebraic manipulation then yields

$$1000/R' = (f/L\eta_r)\Lambda^\circ[t_2^\circ C_m + \underline{C}] \quad (28)$$

where $\Lambda^\circ$ is the equivalent conductance of the external electrolyte at the ionic strength in the membrane pore, $C_m + \underline{C}$, and $t_2^\circ$ is the transference number of the counterion in aqueous solution. With $J_v = L_{ve}(-\Delta\Phi)$, combination of Ohm's law and Eqs. (25), (26), and (28) gives the desired result for $J_v$ as $\mu l/hr\ cm^2$,

$$J_v = i_o(9 \cdot 10^9 F/\eta_o)r_p^2(-z_m)C_m[G(\kappa r_p/2) + (f\tau/\eta_r L)(1 + \beta\tau)^{-1}]/\{\Lambda^\circ(t_2^\circ C_m + \underline{C})\} \quad (29)$$

where $i_o$ is the current density as $mA/cm^2$, and $\eta_o$ is the viscosity of pure water. The term in curly braces is essentially the specific conductivity of the electrolyte solution in the pore.

Using the Stokes–Einstein relationship for the tracer diffusion coefficient, $D_1^* = kT/6\pi\eta a$, where "$a$" is the Stokes radius of the diffusing solute, and $k$ is Boltzmann's constant, combination of Eq. (10) and Eq. (25) yields the theoretical expression for the flux enhancement parameter, $\alpha$, for a given pore or a collection of identical pores,

$$\alpha = [F(-\Delta\Phi)/RT]\{z_1 + 1.5\pi \cdot 10^{-3}N_o a r_p^2(-z_m) \times C_m[G(\kappa r_p/2) + (f\tau/\eta_r L)(1 + \beta\tau)^{-1}]\} \quad (30)$$

where $N_o$ is Avogadro's number, $-\Delta\Phi$ is the potential drop across the membrane as volts, $F$ is Faraday's constant as coulombs/Eq, $RT$ is joules/mol, and $C_m$ and $\underline{C}$ are molar concentrations of fixed charges and co-ion, respectively, in the pore.

### Magnitude of the Barry–Hope Induced Osmotic Effect

As the following argument will show, the induced osmotic pressure effect contributes little in transdermal applications. The thickness of the unstirred layer, $\tau$, in our electroosmotic flow experiments (11) is about 0.08 cm due to the use of the steel support plates. A value of the same magnitude seems plausible for an unstirred *in vivo* application. The value of $\tau$ is certainly less in the typical *in vitro* iontophoresis experiment (some stirring), values of the order of $10^{-2}$ cm being representative (18). Thus, the induced osmotic pressure effect is extremely small, contributing only about 5% to the measured volume flow in our electroosmotic flow experiments (11) with HMS and being entirely negligible in a typical *in vitro* iontophoresis experiment. Noting that the direct current resistance of fully hydrated human skin following iontophoresis is about a factor of 10 greater than similarly treated HMS (19,20), Eq. (28) indicates tht the term, $(f/L\eta_r)$, for human skin is about 1/10 that for HMS, and therefore, the induced osmotic effect is also about one order of magnitude smaller. Thus, contrary to the observations made by Barry and Hope (8,9) for plant cell membranes, volume flow in transdermal applications is essentially independent of the induced osmotic pressure effect.

### Evidence for Pore Heterogeneity in Hairless Mouse Skin

The theoretical results given to this point apply either to a given pore or to a collection of pores identical in charge concentration. The theoretical results for electrical resistance, transference number, and $L_{ve}$ do not appear consistent with the corresponding data (11) unless hairless mouse skin is composed of pores varying in size, with the larger pores having a much higher concentration of fixed negative charges. We now show that the assumption of a single value for $C_m$ for all pores leads to inconsistency. The membrane charge concentration, $C_m$, and pore radius, $r_p$, for hairless mouse skin at pH 8.3 may be estimated using transference number, resistance, and $L_{ve}$ data (11). Calculation of $C_m$ by fitting the transference number data (11), to Eqs. (21) and (22) (with $\lambda_i/\lambda_j = \lambda_i^\circ/\lambda_j^\circ$), gives $C_m \approx 0.013 \pm 0.004$. A value

for $C_m$ as well as the group of terms, $f/\eta_r L$, may be evaluated from electrical resistance data (Ref. 11). Using literature data for conductivity of NaCl at 25°C (13) and $R'$ data for HMS in solutions of varying NaCl concentration (11), regression analysis of Eq. (28) with $\underline{C}$ given by Eq. (21) gives $(f/L\eta_r) = 0.102 \pm 0.002$ cm$^{-1}$, $C_m = 0.29 \pm 0.02$ $M$. Since the conductivity data were at 25°C, $\eta_r$ is relative to water at 25°C. The value of $(f/L\eta_r)$ is not sensitive to the value of $C_m$. Fixing $C_m$ at 0.013 $M$, a fit of the resistance data gives $(f/L\eta_r) = 0.103$, although the fit is poor. The available volume flow data (11) are not sufficiently presise to determine uniquely both $C_m$ and $r_p$. Using the fixed values, $C_m = 0.015$, and $(f/L\eta_r) = 0.10$, a fit of the experimental $L_{ve}$ data (Ref. 11, Fig. 8) to Eqs. (25) and (26) gives $r_p = 70 \pm 8$ Å. However, the observed flux enhancement in the presence of a pure osmotic pressure difference (12) is much too small to be consistent with an average pore size of 70 Å. These osmotic volume flow data suggest a mean pore size for pure osmotic flow of ≈18 Å with an upper limit of ≈25 Å. With $r_p$ fixed at 18 Å, a fit of the $L_{ve}$ data gives $C_m = 0.14 \pm 0.02$. Thus, it appears that a different average value of $C_m$ is demanded by each of the three experiments considered, a result inconsistent with a homogeneous pore system. Comparison of volume flow data with transference number data at pH 4 (11) and nonzero flux of glucose from a cathode donor (12) also are inconsistent with a homogeneous negatively charged pore system.

We now demonstrate that a heterogeneous pore system where the larger pores have a larger negative charge *is* consistent with both the theoretical results and the data. We approximate the actual pore distribution by three types of pores: pore type 1 is positively charged pores with a concentration of 0.3 $M$ and a radius $r_o/2$; pore type 2 is neutral pores (no charge) with radius $r_o$ and pore area fraction arbitrarily set at 0.5; and pore type 3 is negatively charged pores with a charge concentration of 0.3 $M$ and a radius $2r_o$. This model is obviously an approximation, as the pore radii in a real system are not necessarily at the relative size ratio assumed in the model, and the real pore distribution likely contains a great many more than three types of pores. The relative number of each type of pore (pore number fraction) is then determined by a fit of the model to the experimental transference number data (Ref. 11, Fig. 9). The value of $r_o$ is fixed by fitting the mean of the $L_{ve}$ data to the theoretical model. Table I summarizes the results of these calculations. Using the pore distribution model defined by Table I and the appropriate theoretical expressions for resistance [Eq. (28)] and volume flow coefficient [Eq. (25)], resistance and volume flow "data" may be calculated. When these "data" are fitted to Eqs. (22), (25), and (28) (i.e., treating all pores as equivalent) to obtain values of $C_m$, we find that $C_m = 0.24$ from the resistance data, $C_m = 0.11$ from $L_{ve}$ data ($r_p = 21$ Å), and $C_m = 0.013$ from transference number data. The pore distribution model also indicates that the mean pore radius relevant to pure osmotic flow is 1.30 $r_o$ (18 Å), which is consistent with the osmotic flow data (12). The $C_m$ values are very close to the corresponding observed values generated in similar fashion using experimental data (0.29, 0.14, and 0.013, respectively) and, therefore, demonstrate that a heterogeneous pore system can lead to the observed variations in $C_m$.

Table I. Model for Pore Size and Charge Distribution in Hairless Mouse Skin at pH 8.3

| Pore Type | Pore charge ($Z_m$) | $C_m$[a] | Number fraction[b] | $r_i$ (Å)[c] | Area fraction |
|---|---|---|---|---|---|
| 1 | + | 0.3 | 0.604 | 6.75 | 0.218 |
| 2 | 0 | 0.0 | 0.347 | 13.5 | 0.500 |
| 3 | − | 0.3 | 0.0489 | 27.0 | 0.282 |

[a] Magnitude of $C_m$ is selected such that the model is consistent with electrical resistance data.
[b] The number fraction of pore type $i$ is determined by a fit of the model to transference number data.
[c] The pore radii are determined by a fit of the model to volume flow coefficient data, $L_{ve}$.

### Flux Enhancement for a Heterogeneous Pore System

Since the pore distribution defined by Table I is fully consistent with the transference number, volume flow, and electrical resistance data, we assume that this distribution will also give reliable predictions for the flux enhancement ratio. The flux enhancement ratio for the membrane as a whole may be obtained by summing the flow contributions for each type of pore, which gives

$$J_1/J_1^D = \Sigma A_i \alpha_i [1 - \exp(-\alpha_i)]^{-1} \quad (31)$$

where the summation is over all three pores, and $\alpha_i$ is the flux enhancement parameter for each pore type $i$ [Eq. (30)]. The term, $A_i$, is the area fraction effective for transport of pore $i$, defined by

$$A_i = P_i n_i r_i^2 / \Sigma P_i n_i r_i^2 \quad (32)$$

where $n_i$ and $r_i$ are the number fraction and pore radius, respectively, for pore type $i$ (Table I), $P_i$ is the product of the distribution coefficient for species 1 in pore $i$, and the reflection function for component 1 in pore $i$, $P_i = K_1^i(1-\sigma_i)$. The distribution coefficient of component 1 in pore $i$, $K_1^i$, may be related to the electrolyte distribution coefficient for pore $i$, $K_{23}$ ([Eq. (21)] by $K_1^i = (1/K_{23})^{z_1}$. The reflection coefficient for species 1 in pore $i$, $\sigma_i$, cannot be calculated. However, assuming that the pore radius given by the model is close to the actual pore radius, one might reasonably assume that if the Stokes radius of component 1 is significantly larger than the (average) radius for pore type $i$, the reflection coefficient should be close to unity. The passive, or diffusional, flux is given by

$$J_1^D = (\langle P \rangle)(f/\eta_r L)(kT/6\pi\eta_o a)c_1^\circ \quad (33)$$

where $\langle P \rangle$ is the average value of $P_i$

$$\langle P \rangle = \Sigma P_i n_i r_i^2 / \Sigma n_i r_i^2 \quad (34)$$

Theoretical values of flux enhancement for hairless mouse skin at 37°C with a voltage drop of 1 V are shown in Fig. 2. The calculations are based on the pore distribution model described and the theoretical relations presented [Eq. (31) and all secondary equations]. Calculations are given for anode (+) and cathode (−) delivery of monovalent cations, monovalent anions, and neutral species with Stokes radii of 4 Å (representative of a small molecule the size of mannitol or

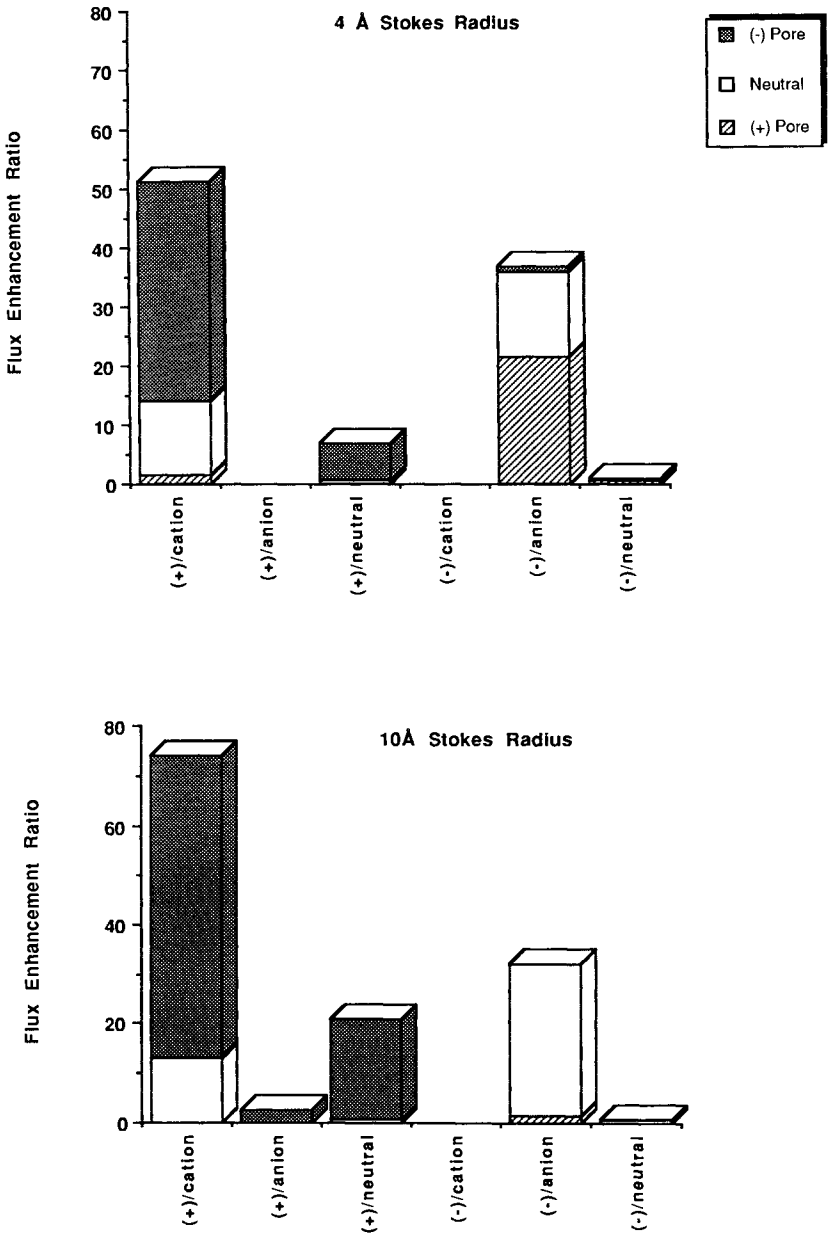


Fig. 2. Flux enhancement ratios for hairless mouse skin in 0.1 *M* NaCl: calculated from the theoretical model for a potential difference of 1 V at 37°C. The horizontal variable is "electrode polarity/permeating species type." The contributions of the three pore types are differentiated by the shading: negatively charged pores, dark shading; neutral pores, unshaded; positively charged pores, light shading. The reflection coefficient is assumed to be 0.97 for 10-Å species in the small (6.75-Å) positively charged pores. All other reflection coefficients are assumed to be zero.

glucose) and 10 Å (representative of a small polymer the size of inulin). The contribution of the negative pores (pore type 3) is given dark shading, the contribution of neutral pores (pore type 2) is unshaded, and the contribution of the positive pores (pore type 1) is given light shading. Since each pore type is probably a distribution of charge concentrations and sizes, the reflection coefficient would not necessarily be unity if the Stokes radius is larger than the mean pore radius, although it should be close to unity. The reflection coefficient for 10 Å species in the positive pores (6.75 Å) is arbitrarily taken as 0.97. All other reflection coefficients are taken as zero.

It may appear surprising that the flux enhancement ratio for cations or neutral species in negative pores *increases* as the size of the transported molecule increases. This is a simple consequence of the fact that flow of a solute with the solvent stream (volume flow) is independent of solute size, whereas flow of solute relative to the solvent stream (diffusion) is inversely proportional to size through the Stokes–Einstein relationship. Of course, the absolute flux may be

extremely small even if the flux enhancement ratio is very large.

As intuitively expected, the flux enhancement ratio is essentially zero for cathodic delivery of cations and anodic delivery of small anions. However, due to a small but significant contribution from the negative pores, the flux enhancement ratio for a large anion delivered from the anode is nonzero (2.7). Here, the large negative effect of the electric field:ion interaction [the $z_1$ term in Eq. (30)] is offset by a slightly larger positive effect of electroosmotic flow [the $C_m$ term in Eq. (30)], and the value of $\alpha_3$ is positive. For small ions the electroosmotic flow effect is not large enough to offset the unfavorable electric field:ion effect. Of course, in cathodic delivery of cations, both the electroosmotic flow and the ion:electric field effects oppose transport in the negative pores, and the flux of cations is essentially zero. Due to small contributions from neutral and positive pores, flux enhancement ratios are roughly unity for cathodic delivery of neutral species.

Since flux via electroosmotic flow is proportional to the product of the pore charge concentration and the square of the pore radius [Eq. (30)], flux enhancement via electroosmotic flow is most significant for the large negative pores. Thus, the largest flux enhancement ratios are for anodic delivery of cations. Here, the electric field:ion interaction effect and the electroosmotic flow effect are both positive. Due to electroosmotic flow opposing transport in the negative pores during cathodic delivery, positive and neutral pores dominate the cathodic delivery of anions. The contribution of positive pores to cathodic delivery of large anions is small because of the high reflection from the small positive pores. It should be noted that while the contribution of neutral pores to cathodic *flux enhancement* is much higher for large anions than for small anions, the term, $\langle P \rangle$, is proportionately smaller for larger species. Thus, the product, $\langle P \rangle \cdot$ (flux enhancement ratio), for neutral pores is the same for both 4- and 10-Å species, and the net flux, $J_1$, is actually smaller for the 10-Å species due to the inverse relationship between diffusion coefficient and size required by the Stokes–Einstein relationship.

As for HMS, the net polarity of the pores in human skin is negative at neutral pH (4,21). For human skin, transference number data (4) at neutral pH may be used to calculate [Eqs. (21) and (22)] a "mean" value for $C_m$ of 0.13, which is a factor of 10 higher than the corresponding $C_m$ for HMS. This result suggests a greater negative charge and/or a greater area fraction of negative pores in human skin. Thus, one might expect [Eq. (29)] greater electroosmotic flow in human skin than in HMS at the same current density and NaCl concentration, provided that the pore sizes in human skin are at least as great as in HMS. Consistent with this speculation, volume flow in human skin (21) is about a factor of 7 greater than in HMS (1 mA/cm$^2$, 0.1 *M* NaCl). Consequently, one would expect that the flux enhancement ratio for anodic delivery of a neutral species in human skin would be about a factor of 7 greater than the corresponding flux enhancement ratio in HMS.

## DISCUSSION

While the theoretical analysis is based on a very simple model which cannot be an exact representation of iontophoresis in biological membranes, the procedure of evaluating key parameters from experimental data does impose experimental constraints on the theory. Since the parameterization is based on "initial" volume flow data (11) and electrical resistance measured at 1 mA/cm$^2$, application of the theory to significantly different current densities and long iontophoresis times involves the implicit assumption that the pore characteristics (Table I) remain constant. Yet properties of HMS do depend on current density and time (11). In quantitative applications of the theory, the only practical procedure is to assume that such variations may be attributed to changes in $f/L\eta_r$. Electrical resistance data may be used to estimate $f/L\eta_r$ as well as calculate the appropriate value of voltage drop in a constant-current experiment, thereby allowing extension of the theory to experimental conditions beyond those of the parameterization experiments (12). The available electrical resistance and volume flow data (11) are consistent with this procedure, although most of these data are limited to a narrow current density range (1–2 mA/cm$^2$). Thus, with the possible exception of experiments involving very high or very low current densities, the parameterized theory should be at least a semiquantitative representation of transdermal iontophoresis in HMS, although due to defects in the theory, the values of the parameters [$f/L\eta_r$, $r_o$, and $C_m$] may not correspond exactly with their intended meaning. A detailed comparison of experimental and theoretical fluxes in HMS is given in part III of this series (12). In general, the theoretical results are in quantitative agreement with experiment. While the mathematical relations and the concept of a heterogeneous pore charge distribution are not restricted to HMS, additional data are needed to parameterize the theory for *quantitative* application to membranes other than HMS. The theoretical calculations (Fig. 2) do appear at least qualitatively consistent with experimental observations on depilatated mouse skin (2) and human skin (4).

The parameters are consistent with the concept that iontophoretic transport occurs primarily through aqueous shunt pathways (3,4,19,20) or "pores." However, there appears to be a much greater number of pores than the number of hair follicles and sweat ducts. The density of pores (number/cm$^2$) may be estimated from the pore distribution model (Table I) and the pore area fraction, $f$. Assuming $\eta_r \approx 1$, and taking 25 μm for the thickness ($L$) of the hydrated stratum corneum of HMS (22,23), values of "$f$" are evaluated from the respective values of ($f/L\eta_r$). With $r_3 = 27$ Å, the pore density of large negative pores in HMS is calculated at $\approx 3 \cdot 10^8$ cm$^{-2}$. It should be noted that the calculated density of aqueous pores is about a factor of $10^6$ greater than the corresponding density of hair follicles (22). Of course, if one makes the questionable assumption that the relative viscosity is of the order of $10^6$, the pore density and hair follicle density would be roughly equal. Note also that the calculated pore radius (27 Å) is much smaller than the radius of a hair follicle (46 μm).

It should be emphasized that the flux enhancement theory developed in this report addresses the case where the drug either is uncharged or, if an electrolyte, is present at concentrations low relative to the concentration of supporting electrolyte. The other extreme, where the drug is an

electrolyte (ionic components 1 and 4) present at high concentrations and therefore carries most of the current, is a much simpler theoretical problem. Here the drug essentially becomes the supporting electrolyte. Electroosmotic flow is only a small pertubation on the ionic flux and may be ignored as a first approximation, Thus, the flux of component 1 is given by

$$J_1 = t_1[i/F|z_1|], \tag{35}$$

where $i$ is the current density, $F$ is Faraday's constant, $z_1$ is the charge on component 1, and $t_1$ is the transference number of ionic component 1. The transference number of the counterion component (i.e., either component 1 or component 4) may be estimated from Eq. (22), where $\underline{C}$ refers to the molar concentration of drug in the pores, and $C_m$ is the "transference number average" pore concentration of negative charge (0.013 $M$ for HMS and 0.13 $M$ for human skin). Allowing for nonzero reflection coefficients, the ratio of single ion conductivities in the membrane phase is taken as the product of corresponding conductivity ratio in the external solution and the ratio of reflection coefficient functions $(1-\sigma)$. It should be noted that the potential for variability in flux is much less when the drug is present in great excess than when the drug carries only a small fraction of the current. At constant current, the only parameter in Eq. (35) subject to variation is the transference number. Assuming small reflection coefficients, the only potential variable is $C_m$, and particularly at high electrolyte concentration, variations in $C_m$ have little effect on the transference number.

In summary, the proposed theoretical model appears to be both self-consistent and consistent with the available experimental data. Although the model is an oversimplified representation of reality, the theory probably has sufficient validity to serve as a useful "baseline" to aid in the interpretation of mass transfer in iontophoresis.

## REFERENCES


1. P. Tyle. *Pharm. Res.* 3:318–326 (1986).
2. L. Gangarosa, N. Park, C. Wiggins, and J. Hill. *J. Pharmacol. Exp. Ther.* 212:377–381 (1980).
3. R. Burnette and D. Marrero. *J. Pharm. Sci.* 75:738–743 (1986).
4. R. Burnette and B. Ongpipattanakul. *J. Pharm. Sci.* 76:765–773 (1987).
5. D. G. Miller. *Chem. Rev.* 60:15–37 (1960).
6. N. Lakshminarayanaiah. *Chem. Rev.* 65:491–565 (1965).
7. Y. Kobatake, M. Yuasa, and H. Fujita. *J. Phys. Chem.* 72:1752–1757 (1968).
8. P. H. Barry and A. B. Hope. *Biophys. J.* 9:700–728 (1969).
9. P. H. Barry and A. B. Hope. *Biophys. J.* 9:729–757 (1969).
10. J. C. Keister and G. B. Kasting. *J. Membr. Sci.* 29:155–167 (1986).
11. M. J. Pikal and S. Shah. *Pharm. Res.* 7(3):213–221 (1990).
12. M. J. Pikal and S. Shah. *Pharm. Res.* 7(3):222–229 (1990).
13. D. G. Miller. *J. Phys. Chem.* 70:2639–2659 (1966).
14. M. J. Pikal. *J. Phys. Chem.* 75:3124–3134 (1971).
15. A. W. Adamson. *Physical Chemistry of Surfaces,* 2nd ed., Interscience, New York, 1967, pp. 209–214.
16. G. S. Manning. *J. Chem. Phys.* 46:4976–4980 (1967).
17. R. B. Bird, W. E. Stewart, and E. N. Lightfoot. *Transport Phenomena,* John Wiley & Sons, New York, 1960, pp. 43–47.
18. K. Valia and Y. Chen. *Drug Dev. Ind. Pharm.* 10:575–599 (1984).
19. R. R. Burnette and B. Ongpipattanakul. *J. Pharm. Sci.* 77:132–137 (1988).
20. R. R. Burnette and T. M. Bagniefski. *J. Pharm. Sci.* 77:492–497 (1988).
21. H. Rein. *Z. Biol.* 81:125–140 (1924).
22. R. L. Bronaugh, R. F. Stewart, and E. R. Congdon. *Toxicol. Appl. Pharmacol.* 62:481–488 (1982).
23. B. Idson. *J. Pharm. Sci.* 64:901–924 (1975).